Tribology International 125 (2018) 17–26

Contents lists available at ScienceDirect

Tribology International

journal homepage: www.elsevier.com/locate/triboint

Experimental and theoretical studies of the dynamic behavior of a spiral-groove dry gas seal at high-speeds

Yuan Chen, Xudong Peng*, Jinbo Jiang, Xiangkai Meng, Jiyun Li

College of Mechanical Engineering, Zhejiang University of Technology, Hangzhou, 310032, China

ARTICLE INFO

Keywords:
High speed
Dry gas seal
Spiral groove
Dynamic behavior

ABSTRACT

Because of great axial vibration of the rotor system, dry gas seal has a big film thickness disturbance, which may cause contact rubbing of seal faces or excessive leakage. Focusing on this problem, experimental studies on transient-state film thickness and leakage rate of a spiral groove dry gas seal at high-speeds are carried out under different spring pressures and different spiral groove depths. And the experimental results of film thickness disturbance and average leakage rate are predicted by perturbation method and gas lubrication theory. Results show that the theoretical results of variation trends of film thickness disturbance amplitudes coincide well with the experimental data, and it also represents that the perturbation method is an effective forecasting method in dynamic analysis.

1. Introduction

It is well known that a spiral groove dry gas seal (S-DGS) is widely used in centrifugal compressor because of its superior sealing performance [1,2]. But with the centrifugal compressor developing toward the larger size diameters of shaft and high rotation speed conditions, the S-DGS has exposed a relatively worse disturbance-resist ability. So it is of important significance to deeply understand dynamic behavior based on theoretical and experimental analyses for getting a better design guide to a high-speed S-DGS.

There have been a lot of research works about the dynamic theory of non-contacting mechanical seals since 1980s, but from the recent studies [3–6], one of the clearest signs that the dynamic theory still has a long way to go because there are a lot of complicated factors should been taken into account with the development of the theory research level. At present, the methods of theory analysis main include direct numerical simulation method, perturbation method, step jump method and direct numerical frequency response method [7]. And the perturbation method, which can obtain numerical results with suitable accuracy and has a high computational efficiency, is adopted widely by scholars in the field of dynamics research of a non-contacting mechanical seal [8–14].

The theoretical researches can hardly do without experimental verification. Meanwhile, relatively backward dynamics theory makes it hard to predict exactly the practical dynamic behavior of the non-contacting mechanical seal. In this case, experimental study of dynamic behavior of a mechanical seal has been a major focus in order to satisfy the needs of engineering design. Etsion et al. [15,16] were perhaps the first researchers to set up dynamic performance experiment rig of non-contacting mechanical seal with flexibly mounted stator (FMS). In their experiments, three proximity probes were respectively used to monitor the motions of seal rings, and the phenomenon of self-excited oscillation and large amplitude wobble had been found. In addition, Metcalfe [17] found that there was a half-frequency whirl when flexibly mounted stator tends to follow rotor angular misalignment. Lee and Green [18,19] further researched the steady and dynamic state response by their test rig of non-contacting mechanical seal with flexibly mounted rotor (FMR). The results of experiment showed that the system nonlinearities can cause higher harmonic oscillations and a high relative angular misalignment between the seal faces can cause rubbing contact, but to maximize the fluid film stiffness by the combination of the seal parameters is optimal way for safe non-contacting operation. Later, Zou et al. [20–22] used the same test rig designed by Lee and Green to make a systematic studies on dynamic responses of axial and angular modes, and they tried to eliminate face contact through reducing the maximum relative misalignment between seal faces. Furthermore, Green [23] changed the fluid film stiffness and damping coefficients by governing closing force so that the dynamic behavior of mechanical seals can be monitored and controlled real-time.

There are already lots of experimental studies on dynamics of non-contacting mechanical seals in recent decades, but it is relatively scarce researches about dynamics of DGS, especially about the influence of gas film dynamic characteristics on the dynamic behavior of S-DGS at high-speeds. In this paper, a test rig is developed, and the experimental and

* Corresponding author.
E-mail addresses: xdpeng@zjut.edu.cn, xdpeng@126.com (X. Peng).

https://doi.org/10.1016/j.triboint.2018.04.005
Received 5 February 2018; Received in revised form 30 March 2018; Accepted 7 April 2018
Available online 09 April 2018
0301-679X/

Nomenclature

A_{rz}	axial excitation amplitude
c_s	secondary seal damping
c_{zz}	gas film dynamic damping
d	displacement of the probe of surface profile instrument
h	transient-state gas film thickness
h_{ave}	average value of film thickness in stage of stably running
h_b	equilibrium film thickness in non-groove
h_g	groove depth
$h_{g,ave}$	average value of groove depth
h_i	film thickness at the i-th collection point
Δh_q	root-mean-square amplitude of film thickness disturbance
h_0	equilibrium film thickness in seal face
k_s	spring stiffness
k_{zz}	gas film dynamic stiffness
m	stator mass
N_g	number of groove
N	collection number of experiment data
n	rotational speed of shaft
P	transient-state gas film pressure
p_i	pressure at inner radius
p_{out}	pressure at outer radius (sealed pressure)
p_z	perturbation pressure about z axis
p_0	steady-state pressure
Q	transient-state volume leakage rate
Q_{ave}	average value of volume leakage rate
Q_0	steady-state volume leakage rate
r_i	inner radius of seal face
r_g	groove bottom radius
r_o	outer radius of seal face
t	time
z	stator's axial response motion
z_r	stator's axial excitation motion
μ	dynamic viscosity
Ω	angular velocity of shaft
ω	axial excitation motion angular frequency
κ	groove-to-land ratio
φ	spiral angle
δ	groove-to-dam ratio
Λ	compressibility number
Γ	dimensionless excitation frequency

theoretical studies of the dynamic behavior of a S-DGS have been done. It has an important meaning for guiding anti-vibration design of a DGS.

2. Theoretical models

2.1. Physical models

In process industry, a modern high-speed centrifugal compressor usually use the FMS type of S-DGS. The structure schematic of a FMS type of S-DGS is shown in Fig. 1. When the rotor revolves at high speeds, gas film hydrodynamic pressure will be generated by spiral grooves, which will help to separate the two seal faces and maintain a gas film of up to several micron thickness. In the practical running process of a S-DGS, the film thickness has a disturbance caused by the rotor's axial vibration, and a big film thickness disturbance will lead to contact rubbing of seal faces or excessive leakage. Fig. 2 shows the kinematic model of the FMS type of S-DGS. In the dynamic tracking property analysis, the thin gas film, which has certain dynamic stiffness and damping properties, is usually treated as a spring-damper system [8].

2.2. Mathematical models

Assuming the ideal gas behavior for the sealed gas, and the isothermal faces, the transient-state compressible Reynolds equation, which governing the pressure distribution of the gas film, expressed in the polar coordinates is given by Ref. [24]:

$$\frac{1}{r^2}\frac{\partial}{\partial\theta}\left(\frac{ph^3}{12\mu}\frac{\partial p}{\partial\theta}\right)+\frac{1}{r}\frac{\partial}{\partial r}\left(r\frac{ph^3}{12\mu}\frac{\partial p}{\partial r}\right)=\frac{\Omega}{2}\frac{\partial(ph)}{\partial\theta}+\frac{\partial(ph)}{\partial t} \tag{1}$$

The steady-state compressible Reynolds equation expressed in the polar coordinates is given by:

$$\frac{1}{r^2}\frac{\partial}{\partial\theta}\left(\frac{p_0h_0^3}{12\mu}\frac{\partial p_0}{\partial\theta}\right)+\frac{1}{r}\frac{\partial}{\partial r}\left(r\frac{p_0h_0^3}{12\mu}\frac{\partial p_0}{\partial r}\right)=\frac{\Omega}{2}\frac{\partial(p_0h_0)}{\partial\theta} \tag{2}$$

The perturbation compressible Reynolds equations are obtained based on Eqs. (1) and (2) by using perturbation method (the theoretical derivation refers to Ref. [8]). To facilitate the theoretical analysis, the dimensionless variables as follows are introduced:

$$P_0=\frac{p_0}{p_i};\ P_{zj}=\frac{p_{zj}h_b}{p_i}(j=r,\ i);\ \Lambda=\frac{6\mu\Omega r_i^2}{p_ih_b^2};\ H_0=\frac{h_0}{h_b};\ \Gamma=\frac{\omega}{\Omega};\ R=\frac{r}{r_i} \tag{3}$$

The expressions of dimensionless steady-state compressible Reynolds equation and dimensionless perturbation compressible Reynolds equations are shown in Eqs. (4) and (5a)- (5b) respectively:

$$\frac{1}{R^2}\frac{\partial}{\partial\theta}\left(P_0H_0^3\frac{\partial P_0}{\partial\theta}\right)+\frac{1}{R}\frac{\partial}{\partial R}\left(RP_0H_0^3\frac{\partial P_0}{\partial R}\right)=\Lambda\frac{\partial(P_0H_0)}{\partial\theta} \tag{4}$$

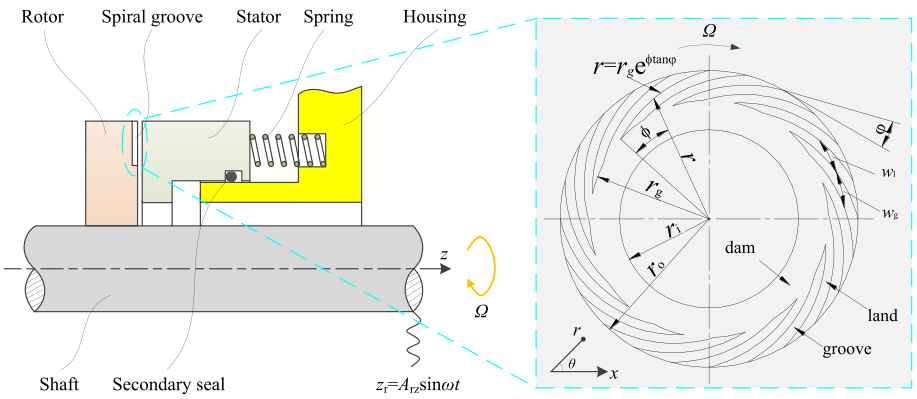

Fig. 1. Structure schematic of a FMS type of S-DGS.